International Journal of Thermophysics, Vol. 12, No. 4, 1991

A High-Accuracy Dilatometer for the Range −20 to 700°C[1]

R. E. Edsinger[2] and J. F. Schooley[2]

We have constructed a linear-thermal expansion apparatus that employs a potassium-loaded heat pipe to provide a homogeneous temperature environment for the sample and utilizes the Merritt–Saunders (optical interferometric) method of observing its expansion. The apparatus is similar in many respects to one described previously. Temperature regulation and measurement are accomplished through the use of a dedicated laboratory microcomputer operating with a simple program. Two platinum resistance thermometers, read automatically by a digital resistance bridge, provide, on command, both the temperature of the heat pipe and that of the sample chamber. Changes in sample length are determined from measurements of the corresponding changes of optical fringes from a Fizeau interferometer as recorded on film. The coefficients of thermal expansion of two Pt–Rh alloy samples determined using the present apparatus agree at the ±2 ppm level with those determined for a similar sample using the previous apparatus.

KEY WORDS: dilatometry; heat pipe; linear thermal expansion; thermometry.

1. INTRODUCTION

More than a decade ago, Guildner and Edsinger designed and built a dilatometer for the accurate determination of the thermal expansion of materials from which their gas thermometer bulbs had been prepared. Based upon the principle of Fizeau interferometry, that apparatus included a sample chamber surrounded by a copper block that was in turn enclosed

[1] Paper presented at the Tenth International Thermal Expansion Symposium, June 6–7, 1989, Boulder, Colorado, U.S.A.

[2] Temperature and Pressure Division, National Institute of Standards and Technology, Gaithersburg, Maryland 20899, U.S.A.

0195-928X/91/0700-0665$06.50/0

within some seven concentric thermal shields [1, 2]. Use of the concentric-shield method for thermal equilibration, coupled with reliance on a calibrated platinum resistance thermometer (PRT) to determine sample temperatures, constituted an advance in high-temperature dilatometric technique over the usual method employed for sample thermometry, even with Fizeau interferometer dilatometers, that involved less-accurate thermocouple sensors [3, 4].

While the linear thermal expansion data obtained with the original apparatus [2] showed fitting precision at the part per million (ppm) level, satisfactory operation of the equipment required the iterative adjustment of nine heater currents. This technique proved to be both time-consuming and tedious. The advent of heat pipes for thermal equilibration led us to rebuild the dilatometer, using a heat pipe instead of multiple shields. The heat pipe operates on the principle of evaporation and condensation of a particular substance that is contained within its walls. "Hot spots" in the enclosed experimental chamber cause local evaporation of the substance, with an accompanying removal of energy equivalent to the heat of evaporation, while "cold spots" cause local condensation and deposit of energy. A wicking material, or a set of grooves, in the interior walls, facilitates the flow of the heat pipe substance.

This paper describes the construction of the new dilatometer and its use to determine the coefficients of linear thermal expansion of a Pt–Rh alloy in the range −20 to 700°C.

2. THERMAL EXPANSION FURNACE

In order to provide linear thermal expansion information adequate for use in the National Institute of Standards and Technology (NIST) Gas Thermometry program, it has been necessary to measure the sample temperature accurately within 0.01°C, while obtaining expansion measurements over the range −20 to 700°C. The success of the previous dilatometer up to 550°C led us to adapt it to the present needs.

Figure 1 shows a schematic drawing of a new thermal expansion furnace. We obtained commercially an Inconel[3] heat pipe (labeled H in Fig. 1) containing 50 g of potassium metal. The lower end of the heat pipe is closed, providing a Dewar-like configuration. An internal vacuum jacket, VJ, permits control of the gas in the sample chamber.

Inside the vacuum jacket, we placed two copper blocks that are joined

[3] Certain commercially available products are identified herein only for description. No implication is intended that these items are superior to similar ones or that the NIST endorses the use of these products.

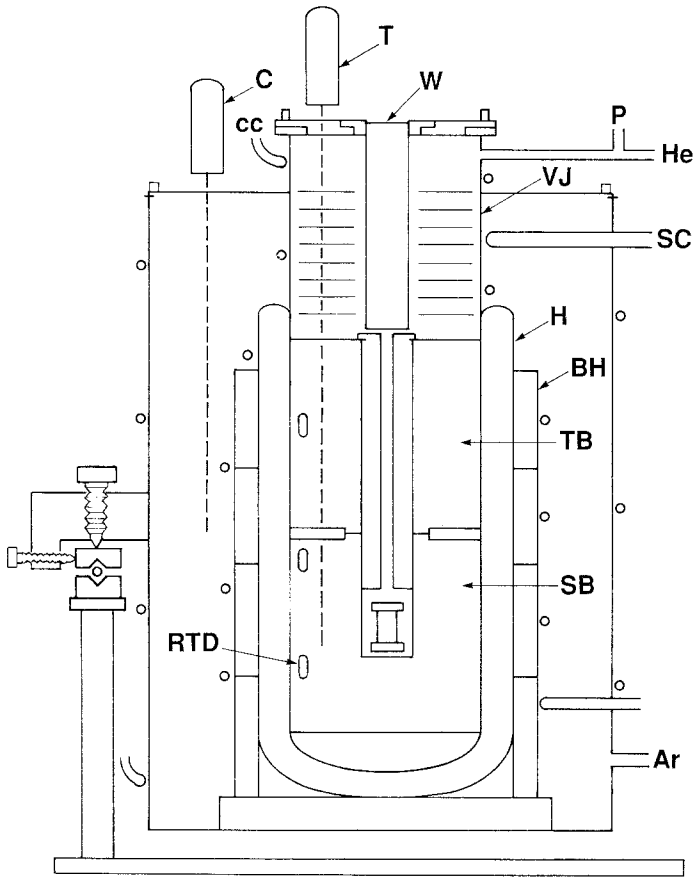

Fig. 1. Schematic drawing of the thermal expansion furnace. A copper cooling coil, cc, is brazed to the brass outer wall. The furnace is supported at three points on a turntable. A closed-end heat pipe, H, heated by four ganged heaters, BH, rests upon an insulating support. A PRT, C, allows rough temperature control. An evacuable sealed tube, VJ, encloses the sample assembly. The lower copper block, SB, encloses the sample and a calibrated PRT, T. The upper copper block, TB, tempers block SB as well as the ^{4}He fill gas, thermometer T, and a central slotted copper block. Three miniature resistance thermometers, RTD, provide temperature uniformity information. A quartz window, W, tempered by a set of baffles, admits light from the interferometer. A coil of stainless-steel tubing, SC, is used to cool the sample chamber. Ports He and P, respectively, admit and monitor the pressure of the fill gas. Port Ar allows filling the furnace with a slight overpressure of Ar gas.

lightly as shown in Fig. 1. The lower copper block, SB, provides a central chamber for the sample assembly and a socket for the long-stem PRT, T, used to determine the sample temperature. On the outside of each copper block is wound a resistance heater. The two block heaters are operated from a single power supply and are connected so that the proportion of heater power in each is variable.

Outside the heat-pipe assembly, a coil of stainless-steel tubing, SC, provides the means of introducing a refrigerant into the furnace to allow measurements below room temperature. Argon gas introduced at a pressure slightly above ambient helps to sweep water and other unwanted impurity gases from inside the furnace.

We selected potassium as the working substance in the heat pipe despite the fact that its vapor pressure becomes substantial only above 400°C, implying that the potassium will not function properly as a thermal equilibrator below that temperature. Given the relatively low radiant heat-transfer properties of the furnace up to that temperature, we expected the heat pipe to serve as a Dewar vessel up to temperatures at which it became active as a thermal element. The ease of control of the furnace and its thermal stability in use over the full range of temperature have proved to be consistent with this interpretation.

3. INTERFEROMETER

Candler [5], Merritt [6], and Saunders [7] have described the use of a Fizeau interferometer for the determination of linear thermal expansion. The configuration of the interferometer sample assembly is shown in Fig. 2.

Interference between the light reflected from the lower surface of the upper fused silica plate of Fig. 2 and that reflected from the upper surface of the lower fused silica plate forms a set of fringes whose centers are separated by a distance

$$z = \lambda_0/\tan\theta \tag{1}$$

where λ_0 is the wavelength of the incident light in vacuum (546.2271 nm for the ^{198}Hg line used in this work [8]) and θ is the angle between the two reflecting surfaces. By careful adjustment of the sample geometry so as to produce an angle of approximately 1′ (see Section 4), a small number of straight fringes could be produced in the field of view of the interferometer. The lower surface of the upper plate was made partially ($\sim$30%) reflecting by coating it with TiO_2; its upper surface was angled at 20′ so that it would reflect light out of the optical path. The upper surface of the lower plate was coated for maximum reflection and its lower surface was roughened.

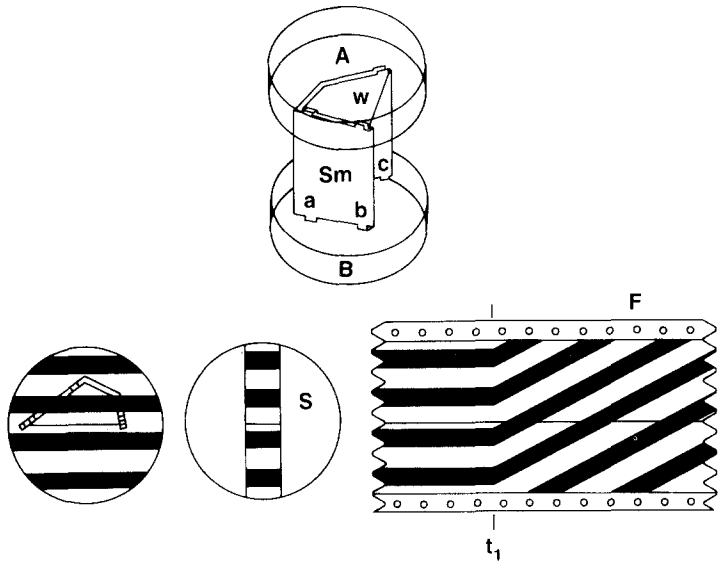

Fig. 2. Sample assembly and fringe pattern. The upper surface of the upper optical plate, A, makes an angle of 20′ with respect to the lower surface, to eliminate its reflections from view. The lower surface of A is coated with TiO_2 for 30% reflection. The upper surface of plate B is coated for total reflection, while its lower surface was left rough. The sample, Sm, is shaped so as to provide three-point support for the upper plate and to produce a fringe pattern similar to that shown in the lower left corner of the drawing. A slot in the central copper tempering block provides a filmed fringe image, S, that is fixed with respect to the fiducial wire, w, during steady-temperature recording. As the temperature changes at time t_1, the film, F, moving leftward, begins to record the moving fringe pattern.

As the temperature of the sample is changed, its length changes and the fringe pattern moves in one direction in response to cooling and in the other direction during heating according to the relation

$$\delta N = (2n\,\delta L)/(\lambda_0) \tag{2}$$

where δN is the change in the total number of fringes at a fiducial mark, n is the index of refraction of the medium, δL is the change in the actual sample length, and λ_0 is the wavelength of the irradiating light.

4. SAMPLE PREPARATION AND ASSEMBLY

The preparation of the samples for these interferometric measurements requires careful work, since the sample must provide a stable support on

which the upper interferometer plate can be placed in a specific position. We first formed the samples into rectangular strips about 25×30 mm and then shaped them into a semicircular or V-shaped configuration as shown in Fig. 2. Then three sets of tabs, a–a, b–b, and c–c, were cut from the horizontal edges of the sample, and a Pt wire was attached so as to connect tabs b and c. Following the cutting, bending, and filing operations, each sample was cleaned and annealed at 1100°C in flowing Ar gas for 1 to 2 h.

Tabs b–b and c–c were prepared so as to be separated by lengths of the sample that were equal within about 0.25 μm. Tabs a–a were left about 1 μm longer than the others, so that, as indicated by Eq. (1), a three- or four-fringe pattern parallel to the Pt-wire fiducial mark (see Fig. 2) was obtained. We used abrasive papers in the range 0.5–30 μm to adjust the heights of the tabs.

We used a calibrated set of gauge blocks, together with a precision micrometer, to measure the dimensions of the sample. By wringing together a stack of gauge blocks selected to approximate the sample height, we could calibrate the precision micrometer within about 0.1 μm.

Once a fringe pattern similar to that shown in Fig. 2 could be observed on viewing the sample-plate assembly in the interferometer light source, the assembly was carefully transferred into the furnace for measurement.

5. FRINGE MEASUREMENT

To obtain the data presented here, the images of the fringes were recorded on film, as indicated in Fig. 2. A small laboratory camera capable of storing about 3 m of 35-mm panchromatic film is mounted at the eyepiece of the interferometer. The film can be moved at three different speeds by a motor-driven sprocket assembly, resulting, upon development, in a streaked image similar to that shown in Fig. 2. Our choices for rate of change of sample temperature and for film drive speed were governed by the light level that was available as well as by the thermal expansivity of the sample.

After developing, fixing, and drying the film, we counted the fringes that passed the fiducial mark between steady-temperature points, so that we could determine the corresponding change in length of the sample. During our measurements, we made sure that we stabilized the sample temperature so that the fringes did not mask the fiducial mark. With the aid of a digital microdensitometer, we could estimate fringe positions within ± 0.001 fringe.

6. COMPUTER-ASSISTED DATA ACQUISITION

Apart from recording the interference fringes, the acquisition of our experimental data was accomplished by the use of a dedicated laboratory microcomputer programmed to accept digital information from a high-accuracy resistance bridge of NIST construction [9] and from a digital voltmeter. Each of these instruments in turn was connected to several sensors, either directly or by means of low-thermal emf scanners. The microcomputer was used also to activate digital-to-analog power supplies to energize the three furnace heater assemblies, to convert resistance values to temperatures, and to convert digital pressure-transducer data from voltage units to pressure units. The ^{4}He pressure thus calculated was further analyzed to yield values of the index of refraction of the sample-chamber gas.

7. TEMPERATURE CONTROL

The sample temperature was reduced to values as low as $-20°C$ by the manually regulated flow of nitrogen gas that had been cooled in a heat exchanger held at $-195°C$ in a bath of liquid nitrogen. As mentioned above, temperatures from ambient to 700°C were attained by regulating the power to band heaters on the heat pipe assembly and to resistive heaters on the upper and lower copper blocks inside the heat pipe.

For regulation of the furnace temperature, our computer program allowed us to enter target temperatures both for the PRT located near the heat pipe (C in Fig. 1) and for PRT T, used to determine the sample temperature. A programmed time interval governed the frequency at which the resistances of these thermometers were measured, the corresponding temperatures calculated, and the information displayed on the terminal and, if desired, printed on the printer. The program compared the target temperatures with those determined by measurement and called for more or less voltage to the heaters depending upon the differences. Limits to the heater voltages could be set by hand; we generally set the heat-pipe target temperature so as to minimize the power to the tempering block and the sample block. In general, these techniques allowed us to obtain stable sample temperatures with less than 30 W of power to the tempering block and 4–10 W to the sample block; in contrast, power to the heat pipe heaters ranged from 10 W at 100°C to about 250 W at 700°C.

8. TEMPERATURE MEASUREMENT

The sample temperature could be evaluated within about $\pm 0.001°C$ in the following manner. Thermometer T was a specially sized PRT, some-

what shorter than usual; it was calibrated according to the International Practical Temperature Scale of 1968 (IPTS-68) and installed in the sample block. The digital resistance bridge permitted the measurement of the resistance of the PRT with a resolution of 1 $\mu\Omega$ on command from the microcomputer. Use of a thermostated resistance standard provided assurance that the bridge measurements were accurate within about 1 ppm. During the times when the furnace temperature was stabilized as described in Section 7, the PRT resistance was read three times, the readings averaged, and the temperature calculated on the basis of the calibration coefficients stored in memory. This process was repeated until the sample temperature appeared to be stable within approximately 0.001°C. Then the industrial-grade thermometer resistances (RTD in Fig. 1), the heater voltages, and the sample-chamber pressure were recorded. PRT T (see Fig. 1) was then monitored again and the temperature was changed at a predetermined rate toward the next temperature.

9. DATA ANALYSIS

In order to analyze our measurements, we adopted the following expression for the length of the sample at any Celsius temperature t_i:

$$L(t_i) = L(t) + \sum \{B_n[t_i^n - t^n]\} \tag{3}$$

where $L(t_i)$ denotes the sample length at temperature t_i, the summation occurs over the range $n = 1$ to $n = m$, and B_n is the coefficient of the t^n term in the sum.

In practice, we measured the length of the sample before installation in the dilatometer within about 5 ppm as described in Section 4. We could express the length in fringes of light in vacuum by use of the relation

$$N_{\text{vac}}(t) = 2L(t)/\lambda_0 \tag{4}$$

where $N_{\text{vac}}(t)$ is the sample length in fringes of light of wavelength λ_0 cm in vacuum and $L(t)$ is the length of the sample (expressed in cm). The value of N thus obtained corresponds to the sample length at the bench-top temperature of the precision micrometer and the gauge blocks; later, this value could be corrected to $t = 0$°C by use of the fitting equations.

We corrected the observed fringe count at the steady-temperature points for the index of refraction of ^{4}He gas, included as a tempering medium in the sample chamber. The 1-atm, 20°C value, 1.000035 [10], was itself corrected to the experimental pressure and temperature by the relation

$$n_i = 1 + 0.000035\,[p_i/101][(293)/(t_i + 273)] \tag{5}$$

with p_i in kPa and t_i in °C. The correction to the vacuum fringe value was then obtained from the relation

$$\delta N(t_i)_{\text{vac-meas}} = 2L(t_i)[1 - n_i]/\lambda_0 \tag{6}$$

where $L(t_i)$ indicates the sample length at temperature t_i.

We fitted the function

$$\Delta N_{\text{vac}}(t_i, t_{i+1}) = \sum \{A_n[t_{i+1}^n - t_i^n]\} \tag{7}$$

to the corrected fringe-temperature data sets. We used a least-squares computational program with up to six coefficients. An F-test analysis of variance procedure was used to select the polynomial which gave the "best fit" at the 95% confidence level [11].

Evaluation of the coefficients A_n permits us to express the linear thermal expansion in the usual form,

$$\begin{aligned} \varepsilon(t, t_0) &= [L(t) - L(t_0)]/L(t_0) \\ &= [N(t) - N(t_0)]/N(t_0) \\ &= \sum \{[A_n/N(t_0)]\, t^n\} \end{aligned} \tag{8}$$

where t_0 denotes 0°C. Note that the factors $[A_n/N(t_0)]$ are the same as the coefficients B_n in Eq. (3).

The thermal expansion can be obtained for any other reference temperature from the relation

$$\varepsilon(t, t_{\text{ref}}) = [\varepsilon(t, t_0) - \varepsilon(t_{\text{ref}}, t_0)]/[1 + \varepsilon(t_{\text{ref}}, t_0)] \tag{9}$$

10. RESULTS

Two thermal expansion samples were prepared from the (80 wt% Pt + 20 wt% Rh) alloy gas thermometer bulb used in recent NIST experiments [12], using the methods described in Section 4. In order to show the level of precision of the thermal expansion measurements obtainable using the dilatometer described herein, we present in Table I the results of measurements taken on one of the samples, labeled S-M, obtained as the sample was cooled in steps from 700 to −20°C, then heated in steps back to 700°C. Prior to the run, the sample length at 23.6°C was found to be 2.528388 cm, or 92,567.3 fringes of light in vacuum. Some 45 fringe differences were obtained on this sample over the range −20 to 700°C. After obtaining preliminary thermal expansion data from other samples of the same alloy, it was found to be unnecessary to record

each time the changing fringe pattern that occurred during a sample temperature change. The fringe differences occurring between the steady temperatures could easily be inferred within one fringe. To these inferred whole fringe values were added fractional fringe counts obtained during steady-temperature conditions. The fractional fringe values were corrected for the refractive index of the medium.

The resulting values of ΔN_{vac} were fitted using Eq. (7). The fitting

Table I. Fitting Parameters for the Thermal Expansion of Sample S-M (80 wt% Pt + 20 wt% Rh)

Equation used in least-squares fitting procedure:

$$\Delta N(t_i, t_{i+1}) = \sum \{A_n(t_{i+1}^n - t_i^n)\} \tag{7}$$

where the summation runs from $n = 1$ to $n = m$

Determination of number of polynomial terms for "best fit": $p = 45$ data points

(1) m	(2) σ^a	(3) F_m^b	(4) $F_{0.95}(1, p-m)$
1	2.169 2	—	
2	0.130 7	12073.4	4.09
3	0.084 7	60.4	4.08
4	0.066 7	26.6	4.08
5	0.061 8	7.8	4.08
6	0.060 4	2.9	4.07

Coefficients of 4th-degree polynomial

n	A_n	σ of A_n
1	0.805 840 5	0.000 897 4
2	0.000 201 509	0.000 005 967
3	−0.000 000 095 958	0.000 000 014 034
4	0.000 000 000 053 023	0.000 000 000 010 233

$N(0°C) = 92{,}548.2$ fringes (calc.)

[a] The estimated standard deviation of the fit.

[b] A factor used to estimate the level of significance of the mth coefficient in the equation fitted to the data. $F_m = 1 + (p - m + 1)[(\sigma_{m-1}/\sigma_m)^2 - 1]$, where p is the number of data points and m is the number of coefficients in the polynomial. The coefficient A_m is considered significant at the desired level of confidence if F_m is greater than the corresponding value given in the column 4. (Entries in column 4 were interpolated from a standard table for the F distribution, e.g., Table III in Ref. 11.)

parameters thus obtained are given in Table I. The standard deviation of the four-term polynomial is somewhat smaller than 0.07 fringe, with the coefficients of the fitting equation as shown in Table I. Using these coefficients, one can calculate a set of ΔN values at the experimental temperatures for comparison with the values ΔN_{vac}. Deviations of the calculated data from the experimental data are shown in Fig. 3. Although inclusion of the t^5 coefficient is statistically significant as judged by our criterion for "best fit," we feel that there is no particular advantage in using a t^5 term in the fitting procedure; on the average, the extra term reduces the differences between the calculated and the experimental values by only 0.005 fringe, a negligible gain.

Table I and Fig. 3 show that the dilatometer used in the present work provides linear thermal expansion values of excellent precision; 90% of the data points shown lie within ± 1 ppm of those calculated with the four-term fitting equation.

The linear thermal expansion for sample S-M can be obtained from Eq. (8), using the coefficients from Table I and the sample length at 0°C;

$$\varepsilon(t, t_0) = 8.707254E\text{-}06\, t + 2.17734E\text{-}09\, t^2 - 1.03684E\text{-}12\, t^3 + 5.7292E\text{-}16\, t^4 \tag{10}$$

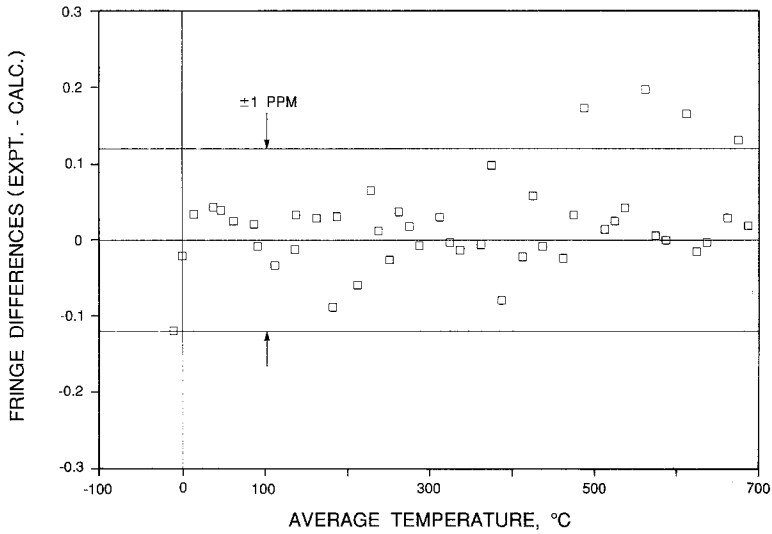

Fig. 3. Differences in fringes of light at 546 nm between the length changes that were observed experimentally for sample S-M (80 wt% Pt + 20 wt% Rh), identified in the text as ΔN_{vac}, and those that were calculated from the fourth-degree fitting equation (see Table I). All data points but one were obtained over at least a 20°C temperature interval. Horizontal lines are drawn at the levels that indicate ± 1 ppm of the sample length.

The linear thermal expansion of the second sample, labeled S-U, was measured in much the same way as S-M, although with fewer (15) steady temperatures. The results, however, were quite similar and were also "best fit" by a four-term polynomial. Figure 4 shows the difference in the thermal expansion calculated from the fitting relation for the two samples from -10 to 700°C. Also shown in Fig. 4 is the thermal expansion difference of a sample of the same composition measured about a decade ago with the use of the dilatometer of Ref. 2. All the results agree throughout the measured ranges within 2 ppm.

The random uncertainty levels of the thermal expansion determinations made with the present dilatometer appear not to exceed 2 ppm. In addition, there are systematic uncertainties whose magnitudes can only be estimated. These include differences between the sample temperature and thermometer T, used to estimate the sample temperature, which we estimate as no larger than 0.001°C; uncertainty in the fringe count, which we estimate as no larger than 0.01 fringe; uncertainty in the actual index of refraction of the gas that occupies the sample space, which we estimate corresponds to no more than 0.02 fringe; uncertainty in the vacuum

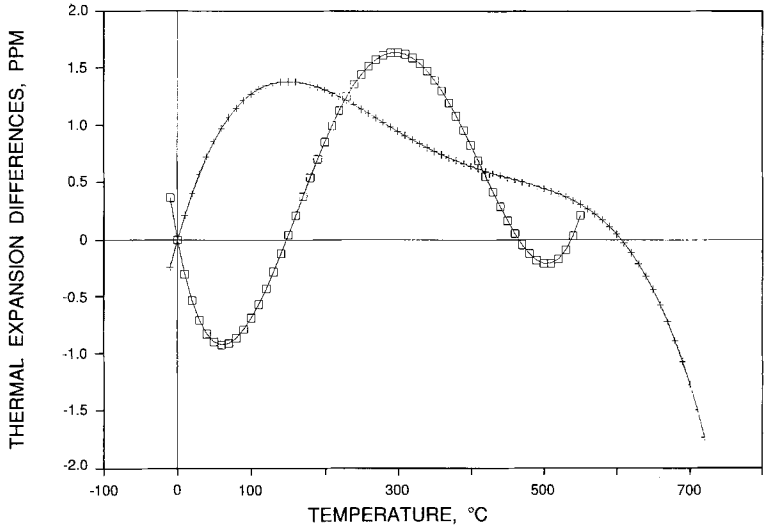

Fig. 4. Differences in calculated linear thermal expansion, $\varepsilon(t, 0°C)$, between the sample in Fig. 3 (sample S-M) and two other samples. Plus signs denote the calculated thermal expansion differences between another sample of the same alloy measured during the course of the experiments described in this report (sample S-U) and sample S-M. Squares indicate the calculated thermal expansion differences between a sample of similar composition that was measured in a dilatometer described earlier [2] and sample S-M.

wavelength of the spectrometer light source, which we estimate to be less than 1 ppm; and changes in the sample thermal expansivity during the measurements, which we estimate as less than 2 ppm by virtue of the agreement between the results obtained on cooling the sample and those obtained on heating.

In summary, we present here a report on an improved dilatometer that is useful in the range −20 to 700°C. It appears capable of providing linear thermal expansion values that are accurate at the level of ±2 ppm of the sample length for samples 2–3 cm in length. Preparation of the samples for observation with the Fizeau interferometer requires considerable care; we can see no shortcut that can obviously eliminate or greatly mitigate this effort. As used in the present work, the dilatometer also involves the tedious use of film recording and measurement of the fringe patterns; however, with the introduction of commercially available linear photodetector arrays, it seems likely that the fringe reading could be accomplished in real time with this instrument.

REFERENCES

1. R. E. Edsinger, 1968 Symposium on Thermal Expansion of Solids, Paper 25, unpublished.
2. R. E. Edsinger, M. L. Reilly, and J. F. Schooley, *J. Res. Natl. Bur. Stand. (U.S.)* **91**:333 (1986).
3. R. K. Kirby, *J. Res. Natl. Bur. Stand. (U.S.)* **71A**:363 (1967).
4. T. A. Hahn, *J. Appl. Phys.* **41**:5096 (1970).
5. C. Candler, *Modern Interferometers* (Hilger & Watts, 1951), Chap. IV.
6. G. E. Merritt, *Scientific Papers of the Bureau of Standards* **19**, No. 485 (1924).
7. J. B. Saunders, NBS Research Paper RP1668, *J. Res. Natl. Bur. Stand. (U.S.)* **35**:157 (1945).
8. V. Kaufman, *J. Opt. Soc. Am.* **52**:866 (1962).
9. R. D. Cutkosky, in *Temperature, Its Measurement and Control in Science and Industry*, **5**, J. F. Schooley, ed. (American Institute of Physics, New York, 1982), p. 711.
10. *American Institute of Physics Handbook*, 3rd ed., D. E. Gray, ed. (McGraw-Hill, New York, 1972).
11. J. Mandel, *The Statistical Analysis of Experimental Data* (Wiley & Sons, New York, 1964), Chap. 8.
12. R. E. Edsinger and J. F. Schooley, *Metrologia* **26**:95 (1989).